Research Article Vol. 34, No. 19 / 21 Sep 2026 / Optics Express 36703
Optics EXPRESS

Ultrafast optical Kerr gate at 1 GHz repetition rate by focusing on bismuth borosilicate (BBS) glass

Amr Farrag,[1] Assegid M. Flatae,[1] Lenorah M. Haight-Stott,[2] Alessandro Iagatti,[3,4] Andrea Lapini,[3,5] Doris Möncke,[2] and Mario Agio[1,3,4,6]

[1]*Laboratory of Nano-Optics, University of Siegen, 57072 Siegen, Germany*
[2]*Inamori School of Engineering at the New York State College of Ceramics, Alfred University, Alfred, NY 14802, USA*
[3]*European Laboratory for Non-Linear Spectroscopy, 50019 Sesto Fiorentino, FI, Italy*
[4]*Istituto Nazionale di Ottica (INO), Consiglio Nazionale delle Ricerche (CNR), 50019 Sesto Fiorentino (FI), Italy*
[5]*Dipartimento di Scienze Chimiche, della Vita e della Sostenibilità Ambientale, Università di Parma, 43124 Parma, PR, Italy*
[6]*mario.agio@uni-siegen.de*

Abstract: The optical Kerr gating (OKG) technique is promising for its high efficiency, broad spectral range, and sub-picosecond temporal resolution, without phase-matching requirements. Traditionally, however, OKG setups have been limited by the need for millijoule-level pulse energies from complex amplifier systems, making them difficult to apply to single emitters. Here, we present an ultrafast OKG scheme using bismuth borosilicate (BBS) glass that operates at a 1 GHz repetition rate under focusing with low pulse energies (<1 nJ) and a gate-pulse peak intensity of ~ 1.20 GW/cm^2. Achieving 175 fs temporal resolution, this microscopy-compatible platform leverages the high nonlinearity and sub-picosecond temporal resolution of BBS glass to enable investigation of ultrafast processes in single quantum emitters.

Published by Optica Publishing Group under the terms of the Creative Commons Attribution 4.0 License. Further distribution of this work must maintain attribution to the author(s) and the published article's title, journal citation, and DOI.

1. Introduction

Measuring ultrafast phenomena lies at the forefront of modern optical science, unlocking new capabilities in fields such as quantum information processing, high-sensitivity detection, and remote sensing [1–4]. Beyond these technological applications, it also serves as a powerful analytical tool for life sciences, enabling investigations at the single-molecule level [5]. However, certain emission processes occur on timescales too short to be resolved with conventional methods, for instance, excited-state dynamics in porphyrins [6] and β-carotene [7]. At the same time, ongoing advances in hybrid quantum systems, where quantum emitters are coupled to nanophotonic structures, show that sub-picosecond emission dynamics are increasingly within experimental reach [8–11]. These developments require advanced ultrafast techniques capable of probing photodynamics at the single-emitter level. To this end, time-resolved ultrafast spectroscopy methods have been developed, such as transient absorption, up-conversion, and optical gating. Yet, to date, these techniques have primarily been applied to molecular ensembles or attenuated laser sources rather than to individual quantum emitters [12–16]. Though recent work has successfully applied transient absorption to individual quantum dots to probe their specific carrier dynamics [17].

#606868 https://doi.org/10.1364/OE.606868
Journal © 2026 Received 9 Jun 2026; revised 28 Aug 2026; accepted 2 Sep 2026; published 18 Sep 2026

Optics EXPRESS

Conventional time-resolved spectroscopy for determining fluorescence lifetimes requires measuring photon emission dynamics following pulsed excitation. Time-Correlated Single Photon Counting (TCSPC) reconstructs decay profiles by accumulating single-photon events over many cycles [18]. The method relies on single-photon-sensitive detectors such as single-photon avalanche diodes (SPADs) or superconducting nanowire single-photon detectors (SNSPDs), whose dead times limit count rates to tens of MHz. While modern TCSPC electronics reach input rates above 1 GHz, the overall temporal resolution, typically a few ps, is constrained by detector jitter and instrument response [18]. Although TCSPC enables picosecond-scale measurements, sub-picosecond processes are still inaccessible. Streak camera–based approaches achieve resolutions down to a few picoseconds and even 100 fs in single-shot mode [19–22], but their bulkiness, cost, and instability at high repetition rates hinder practical use for compact, high-speed single-photon characterization.

Recent advances in stable ultrafast lasers, such as sub-100 fs Ti:sapphire systems, and associated optoelectronic tools have enabled time resolutions comparable to the excitation pulse width through nonlinear optical sampling. Among these, fluorescence up-conversion, based on second-order nonlinear processes in crystals, provides the temporal precision needed to study ultrafast events across the UV to near-infrared range [14,23–29]. This technique achieves resolutions down to 33 fs. However, its dependence on factors such as phase matching, group velocity mismatch, and crystal parameters limits sensitivity and efficiency for single-photon detection, despite recent advances in single-photon frequency upconversion [4].

An alternative and promising nonlinear sampling method, the optical Kerr gate (OKG), sometimes also referred to as optical Kerr shutter (OKS) offers comparable sub-picosecond resolution without requiring phase matching. It is based on the third-order nonlinear Kerr effect and relies on induced birefringence in materials such as Carbon disulfide (CS_2), or fused silica. Time resolutions of 80–100 fs and Kerr efficiencies above 90% have been reported [12,30]. The OKG setup allows temporal gating of fluorescence through polarization rotation, providing ultrafast single-photon detection with high efficiency and broad spectral flexibility. In general, the OKG technique combines high detection efficiency across a broad spectral range. These attributes make it particularly promising for ultrafast single-photon detection, where the emitted signal from a single quantum emitter is inherently weak. In time-resolved techniques based on single-photon detection, acquiring statistically meaningful data requires measurements over a very large number of events to achieve a good signal-to-noise ratio. In this context, developing an OKG technique based on high-repetition-rate lasers would be highly desirable.

Femtosecond GHz repetition lasers are nowadays crucial for various applications, such as high precision metrology via frequency combs [31], ablation of materials in burst-mode [32], and nonlinear optical microscopy [33]. They are highly desirable for modern optical sciences, as it enables faster data acquisition, as well as achieving high signal-to-noise ratio. However, their out-put average powers, limit their usage for studying nonlinear processes, in particular third-order nonlinear optical processes, unless an external amplifier is used, which reduces their repetition rate. This is especially the case with commercial mode-locked Ti:sapphire laser at 1 GHz, emitting in the near infrared (NIR) wavelength range.

In this paper, we demonstrate an ultrafast detection scheme, namely an OKG, with an instrument response function of ~ 175 fs at 1 GHz with less than 1 nJ pulse energy under focusing. This high repetition rate is obtained from a commercial solid-state laser, more than an order of magnitude larger than other solid-state lasers (typically up to 80 MHz) and the pulse energy is nearly six orders of magnitude smaller than amplified systems. This experiment is made possible by appropriately focusing the beam (hence increasing the energy density) [34], despite the shortening of the Rayleigh range, and the high third-order nonlinear response of the BBS glass [35,36].

Optics EXPRESS

2. Materials and methods

2.1. Experimental design

The goal of this work was to implement an ultrafast optical Kerr gate operating at a 1 GHz repetition rate using BBS glass as the nonlinear medium. The experimental approach relied on exploiting the strong third-order nonlinearity of BBS glass under tight focusing conditions to achieve efficient Kerr gating with very low pulse energies.

2.2. Optical Kerr gate principle

In an OKG, a nonlinear medium, so-called Kerr medium, such as in our case BBS glass, is situated between two crossed polarizers. The probe beam does not pass through the second polarizer in the absence of the gate pulse, as the medium remains isotropic (i.e., no birefringence). When the gate pulse arrives, the optical Kerr effect induces a transient birefringence in the medium, rotating the probe beam's polarization. Consequently, a portion of the probe light is transmitted through the second polarizer and can be detected by a photodetector. The detected signal corresponds only to the part of the probe pulse temporally overlapping with the gate pulse.

The transmitted signal as a function of the time delay τ between the pump and probe beam is given by the following relationship:

$$T(\tau) = \int_{-\infty}^{+\infty} I_{\text{probe}}(t-\tau)\sin^2\left(\frac{\Delta\phi}{2}\right)\sin^2(2\theta)\mathrm{d}t, \tag{1}$$

where I_{probe} is the intensity of the probe beam, $\Delta\phi$ is the induced nonlinear phase shift, and θ is the polarization angle between the pump and probe beam, which ideally must be ± 45° to maximize the transmitted signal. The induced nonlinear phase shift $\Delta\phi = 2\pi n_2 L_{\text{eff}} I_{0,\text{ gate}}/\lambda_{\text{probe}}$, where n_2 is the nonlinear refractive index, $I_{0,\text{gate}}$ is the pulse peak intensity of the gate beam, and L_{eff} is the Kerr medium effective thickness, which is calculated as $L_{\text{eff}} = 1 - \exp(-\alpha L) / \alpha$, where α is the absorption coefficient at the wavelength of the gate beam. For a thickness $L = 3$ mm of the BBS glass specimen, and a gate beam at $\lambda_g = 820$ nm, the absorption coefficient will be $\alpha = 120.5\ \text{m}^{-1}$, thus $L_{\text{eff}} = 2.5$ mm.

2.3. BBS glass preparation

The BBS used for our optical Kerr gate experiments is a ternary system composed of Bi_2O_3-B_2O_3-SiO_2 (BBS). Two BBS glass samples were prepared with the following composition: Bi_2O_3 (60 mol%), B_2O_3 (20 mol%), and SiO_2 (20 mol%). Here, the mol% denotes the nominal mole fraction relative to the total moles of all components. This composition was adopted from a previous study on the third-order nonlinear optical properties of BBS glass [35].

Unlike Ref. [35], CeO_2 was excluded, and the glass formation conditions were deliberately modified to minimize coloration. The raw ingredients were melted in a lidded Al_2O_3 crucible at 950 °C for 20 min, followed by pouring the melt into a room temperature graphite mold before annealing at 395 °C for 1 h and slow cooling to room temperature at a rate of ~1 °C/min. The resulting glass samples were cut to ca. 3 mm thick glasses and polished to 1 µm surface quality using a corresponding diamond suspension and microfiber cloth. As the glass was prepared in a small, lab scale batch without a stirrer, convection of the melt and rapid cooling during pouring from the crucible leaves the sample with some density fluctuations that cannot be overcome by annealing or post-synthesis polishing. However, these variations have a negligible effect on focused light transmission.

Optics EXPRESS

2.4. Optical Kerr gate setup

For the nonlinear optical measurements, we employed a tunable ultrafast laser system (Taccor Tune 10, Laser Quantum GmbH) with a tuning range of 730–890 nm, pulse duration < 80 fs, average power of 2.1 W at 800 nm, and a repetition rate of 1 GHz.

For simplicity, a degenerate configuration was used for the probe and gate beams. The setup illustrates the optical layout of the technique. The probe beam passes through a shutter consisting of a nonlinear medium placed between two crossed polarizers. Due to the 1 GHz repetition rate, the gate beam's peak pulse energy is relatively low (less than 1 nJ—nearly 1.20 GW/cm^2 pulse peak intensity, in our case) – a constraint imposed by the Taccor laser's output average power when compared to the amplified pulses used in standard OKG experiments. To enhance the gate efficiency despite this limitation, the probe beam and the pump beams are tightly focused down to 20 μm, and 30 μm, respectively. Accordingly, the Rayleigh range $z_R = \pi\, n\, w_0{}^2 / \lambda$ were calculated for both beams, where n is the linear refractive index and is equal to 2.45 (at 820 nm) for the BBS glass, whilst w_0 is the beam waist. For the probe beam, the $z_R = 0.93$ mm, and for the gate beam $z_R \approx 2$ mm. The physical thickness of 3 mm of the BBS glass specimen was selected based upon formula of Ref. [34], in order to avoid group velocity dispersion (GVD).

2.5. Measurement procedure

The polarization angle between the pump and probe beams was adjusted to 45°, achieved by placing a half-wave plate in the gate beam path. The OKG signal was recorded by measuring the Kerr-rotated probe intensity after the second polarizer (analyzer) as a function of the delay time τ, introduced by varying the optical path length of the pump beam. The pump beam was delayed by the linear translation stage over a distance, corresponding to 1.44×10^{-12} s (1.44 ps) with a maximum temporal resolution of 0.66 fs. Kerr-gated signals were recorded as counts per second integrated over a 1 s acquisition period. The optical bandgap of the BBS glass is obtained from the intercept of the linear portion of the curve with the energy axis. The 110 fs pulse width of the pump (gate) beam was partly measured via the autocorrelator device, and estimated for some other lenses and dielectric mirror, due to the inaccessibility of the measuring device into the OKG part of the setup.

3. Results

3.1. Optical properties of BBS glass

A bismuth borosilicate (BBS) glass specimen was fabricated, shown in Fig. 1(a), and the performed transmission measurements, given in Fig. 1(b), using a standard commercial spectrophotometer (PerkinElmer) confirm that it is transparent in the visible and near-infrared regions.

The spectral measurement shown in Fig. 1(b) indicates that the transmission at λ = 820 nm is nearly 68%, which was obtained using the incoherent light source of the spectrophotometer. Another measurement at the same wavelength was conducted using the femtosecond laser, which shows a linear transmission of nearly 75%. Thus, both measurements imply that the linear absorption range of the BBS glass specimen is between 25-32%.

Before performing the Kerr-gate measurements, it is necessary to assess the presence of self-phase modulation (SPM). This nonlinear effect broadens the input laser spectrum (gate laser beam), generating new frequency components that may overlap with the fluorescence spectrum of the single-photon emitter. Thus, the spectrum of the femtosecond laser centered at 820 nm was measured without the BBS glass and then measured again after inserting the glass into the optical path and subsequently compared to a simulation of the same process. The results indicate that the presence of the BBS glass produces almost no spectral broadening, for more details see Supplement 1.

Optics EXPRESS

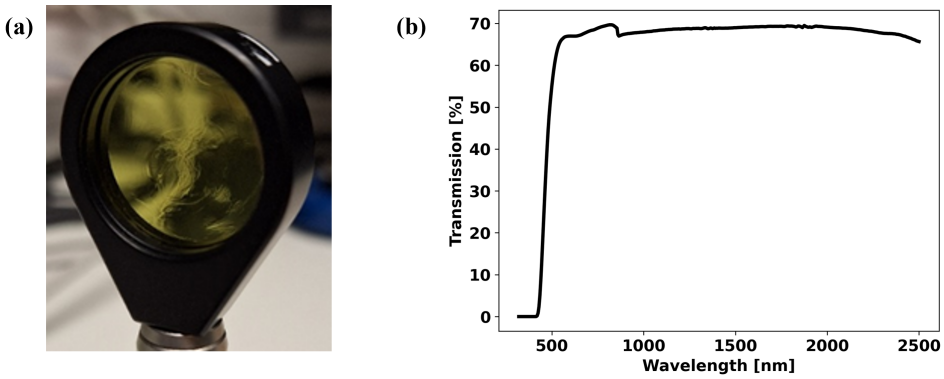

Fig. 1. BBS glass specimen and its transmission spectrum. (A) The 3 mm thick BBS glass specimen. (B) Transmission spectrum of BBS glass (the spectral artefact at 830 nm is due to the spectrophotometer).

3.2. *Kerr gate temporal response*

Degenerate optical Kerr gate experiments were performed using both counter-propagating and co-propagating schemes, with preference given to the counter-propagating configuration to avoid detector saturation due to the pump beam and to minimize noise. The Kerr-rotated probe intensity after the analyzer was recorded as a function of the temporal delay between the pump and probe beams. The scheme of the experimental setup is illustrated in Fig. 2.

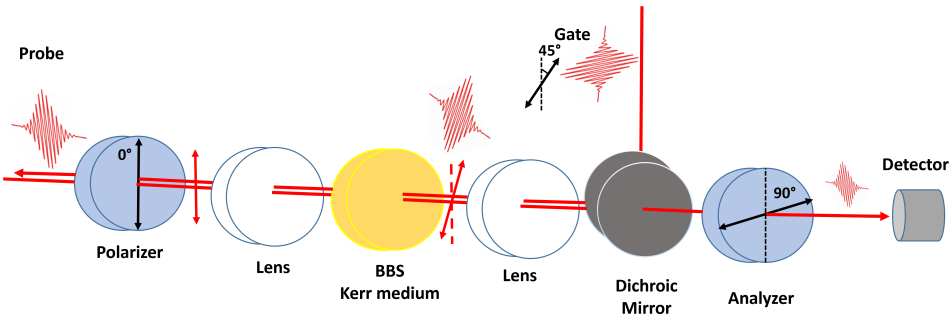

Fig. 2. Optical Kerr gate (OKG) setup. Scheme of the experimental setup for Kerr gate experiment. The gate and probe beams are degenerate at 820 nm, and are counter-propagating. The gate is reflected toward the Kerr medium via a short-pass dichroic mirror. The gate is focused using a 50 mm focal lengths lens to a ~ 30 µm spot, while the probe is focused down to a ~ 20 µm spot using a 100 mm focal length lens.

The resulting temporal profile of the optical Kerr gate signal is shown in Fig. 3, where the x-axis represents the time delay and the y-axis corresponds to the number of counts per second integrated over a 1 s acquisition period. This temporal profile represents the envelope function of the Kerr-gated signal, which was extracted by Fourier analysis from its original OKG time trace, then fitted with a Gaussian function. The full width at half maximum of the fitted Gaussian is 175 ± 1 fs.

The measured temporal profile represents the convolution of the cross-correlation between the gate and probe beams and the nonlinear response time of the BBS glass. This implies that the nonlinear response time of the BBS glass is shorter than 175 fs. For a FWHM of 110 fs for the pump (pulseCheck Autocorrelator, APE GbmH), and estimated similarly for the probe beam for

Optics EXPRESS

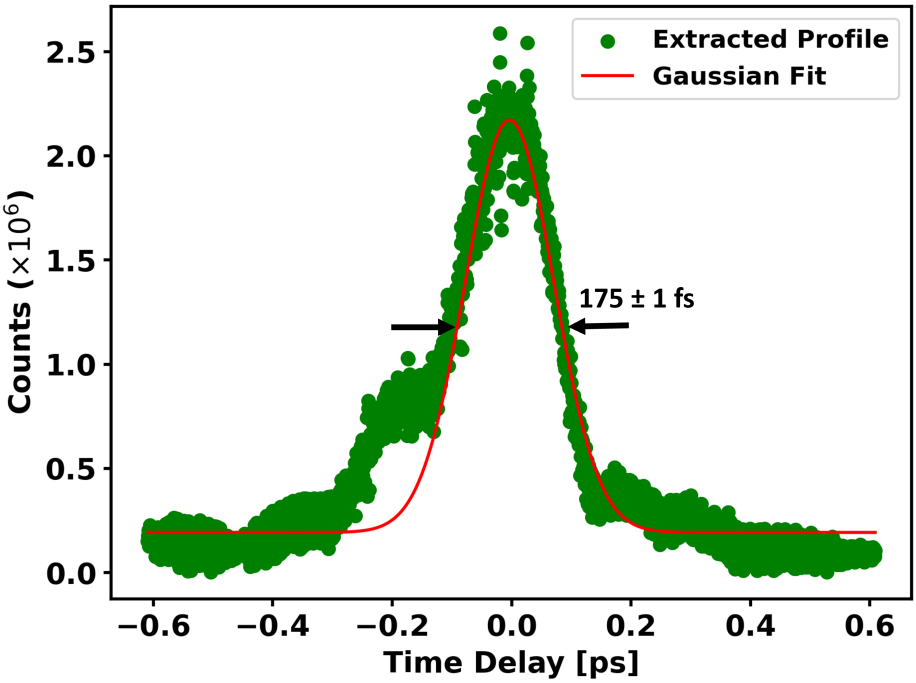

Fig. 3. Temporal profile of OKG of the BBS glass. Temporal profile of OKG signal extracted from its time trace, fitted with a Gaussian function, whose FWHM is 175 ± 1 fs.

simplicity, the expected pump-probe cross-correlation will be about 156 fs. From the measured 175 fs IRF, and assuming Gaussian profiles and using quadratic addition of variances, we can infer that the nonlinear response time is approximately 80 fs. For testing the reproducibility of our results with the Kerr medium (BBS glass specimen), and ensuring its stability against heat accumulation, due to the fs laser irradiation at 1 GHz repetition rate, additional measurements have been taken, some of which we present in the Supplement 1 file. The optical Kerr gate efficiency of the setup was ~ 3%, estimated from an OKG experiment with a CW laser at 656 nm as a probe, and a fs laser at 820 nm as a gate (not shown). This result refers to the percentage increase in the transmitted OKG signal, obtained from 10 spectra of transmitted CW probe spectrum, whose average count rate integrated over the entire CW laser spectrum is 88798 ± 1489 counts/s when the gate is on versus when it is off, which represent the spectrum of the CW probe leakage through the crossed polarizers of a similar number of measurements, whose average count rate also integrated over the entire CW laser spectrum is 86365 ± 1486 counts/s. By subtracting these count rates and dividing them by the average count rate of 86365 counts/s, we obtained the 3% OKG efficiency. The CW experiment was also designed to evaluate the performance of the non-degenerate OKG and to prepare the study of ultrafast fluorescence, which operates at different wavelengths. A shift in the polarization angle corresponding to the maximum transmitted Kerr signal was observed, which was attributed to ellipticity introduced within the optical setup, which is also believed to be the reason for the shoulder appearing at the left-hand side of the temporal profile.

Optics EXPRESS

3.3. Optical bandgap estimation

The optical bandgap of the BBS glass was estimated using the Tauc plot method and from the molar refractivity of the glass. Tauc plots analyze the linear absorption spectrum of the glass, derived from the transmission data as shown in Fig. 4. Linear fitting of the absorption edge yields an optical bandgap energy of $E_g = 2.93$ eV. Further details are provided in the Discussion section.

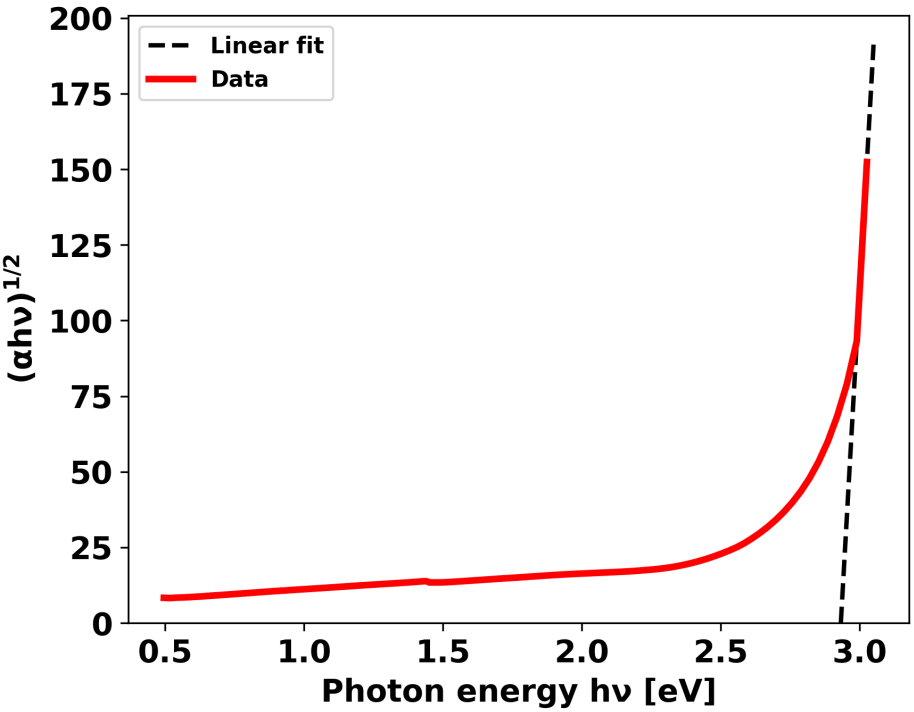

Fig. 4. Tauc plot of BBS glass sample. Here, α represents the absorption coefficient and hυ is the photon energy; the $(\alpha h\upsilon)^{1/2}$ relation indicates an indirect allowed transition. Linear fitting of the Tauc plot of the BBS glass sample that contains 60 mol.% Bi_2O_3. This linear fit interception point with x-axis shows that our BBS glass has $E_g = 2.93$ eV.

Tauc plots notoriously underestimate the band gap, as the Urbach tail, due to charge transfer transitions of impurities shift the observed UV-Vis cut-off in glasses to lower energies compared to the intrinsic cut-off. Using instead the relationship between molar refractivity and bandgap, as discussed by Dimitrov and Komatsu [37,38], more accurate value of the optical bandgap E_g can be obtained. Based on the Lorentz-Lorenz equation, the molar refraction R_m (cm^3/mol.) can be derived from refractive index n and molar volume V_m data and can be related via an empirical formula directly to the intrinsic bandgap, as suggested by Duffy [39] in his discussion of the optical basicity:

$$R_m = V_m \frac{n^2 - 1}{n^2 + 2} = V_m \left(1 - \sqrt{\frac{E_g}{20}}\right) \tag{2}$$

Using a refractive index of 2.45 for BBS and a density of 7.277 g/cm^2 [40], the equation can be rewritten to be

$$E_g = 20\left[1 - \left[\frac{n^2 - 1}{n^2 + 2}\right]\right]^2 = 2.821\ eV \tag{3}$$

Optics EXPRESS

4. Discussion

The results demonstrate that an ultrafast detection scheme based on the third-order nonlinearity of BBS glass can operate at a repetition rate of 1 GHz under focusing, with less than 1 nJ pulse energy, while achieving an instrument response function with a time resolution of 175 fs. This repetition rate enables better signal-to-noise (S/N) ratio, and faster data acquisition, being an order of magnitude larger than the repetition rate from typical commercial solid-state lasers. This will allow to examine a single quantum-emitter with sub-ps time resolution. It also uses a gate pulse energy, that is nearly six orders of magnitude smaller than those obtained from amplified laser systems. This will pave the way for the nonlinear optical community to explore third-order nonlinear optical processes at such high repetition rates and power levels, without the need for integrated- or fiber-optics [41].

The nonlinear optical properties of BBS glass, investigated using a degenerate optical Kerr gate, were previously studied by Lin et al. [42] with a 30-fs laser at 800 nm and a repetition rate of 1 kHz. The nonlinear refractive index was estimated to be $n_2 = 1.6 \times 10^{-14}$ cm^2/W. Furthermore, the nonlinear response time of BBS glass was estimated to be below 90 fs, significantly shorter than that of other materials such as CS_2. In another study, Ref. [35], BBS glass was examined using degenerate four-wave mixing (DFWM) with a 200-fs laser at 810 nm and a 200 kHz repetition rate. The measured ultrafast response time was < 200 fs, in excellent agreement with earlier results from the same research group [36]. They also demonstrated an optical Kerr shutter [43] employing BBS glass as the Kerr medium for optical switching using a 1.5 THz gate beam, achieving a response time of < 150 fs. Additionally, Tan et al. [44] utilized BBS glass as the Kerr medium in a nondegenerate optical Kerr gate for gating spectra from a chirped supercontinuum generated in a sapphire plate. The ultrafast response time of BBS glass in their study, reported as < 85 fs, further confirms its superior temporal resolution compared to materials like CS_2.

Beyond photoinduced birefringence, degenerate OKG experiments often involve self-diffraction via a laser-induced transient grating (LITG). This third-order process occurs when coherent, parallel-polarized pulses create a spatial energy modulation in the medium. Crucially, the LITG signal reflects the pulse correlation time rather than the medium's nonlinear response time. Yan et al. [45] demonstrated that in materials like BBS glass—where the ultrafast electronic response (due to electron cloud distortion) is faster than the pulse width—the OKG signal and self-diffraction become practically inseparable. Consequently, distinguishing between these two effects is essential to accurately characterize the medium's ultrafast response. However, their work showed that at small pump powers, the transmitted signal follows consistently the anticipated OKG behavior.

For applications requiring the detection of extremely weak signals, such as ultrafast single-photon sources, detailed knowledge of the nonlinear material's physical properties is indispensable as the efficiency is critical. One key parameter is the two-photon absorption (TPA) of BBS glass. Linear absorption occurs when the excitation light frequency is resonant with real electronic states. In contrast, within a transparent spectral region far from resonance, two photons can be simultaneously absorbed if the photon density is sufficiently high, a condition typically satisfied within the focal volume of an intense laser beam. When considering nonlinear optical absorption processes such as TPA, the imaginary part of the third-order susceptibility must be considered. Hasegawa et al. [46] measured the nonlinear two-photon absorption coefficient (β) of a bismuth-containing glass (65.5 mol. % B_2O_3) using the Z-scan technique and reported $\beta = 0.8$ cm/GW at 769 nm. Similarly, Zhang et al. [47] employed the same technique to study a ternary Bi_2O_3-rich glass system, Bi_2O_3–B_2O_3–WO_3 (BBW), and reported β values ranging from 0.254 cm/GW to 0.345 cm/GW for a series of samples with varying WO_3 content. The higher β value corresponded to the composition with the greatest WO_3 concentration, while the lower value was observed for the sample with the least WO_3 content.

Optics EXPRESS

Two-photon absorption (TPA) must be carefully considered for three primary reasons. First, at high intensities, nonlinear absorption reduces the effective light available to induce refractive index changes, diminishing process efficiency. Second, TPA and linear absorption can lead to autofluorescence from the BBS glass that can hinder the detection of weak probe signals; however, we irradiated our specimen using the gate beam at 820 nm, and measured the spectrum filtered via a short-pass filter at 800 nm, and found no signs of autofluorescence backgrounds, even though the integration time was 20 s. Third, when using high-repetition-rate lasers like the 1 GHz, even minimal TPA and linear absorption can lead to significant heat accumulation, forming the so-called thermal lensing. The resulting thermal lens acts as a diverging lens that counteracts Kerr-induced self-focusing and optical beam focusing, limiting intensity-dependent phenomena such as optical Kerr gating. Given that our laser operates an order of magnitude faster than standard commercial systems, investigating TPA in BBS glass is essential. The presence of TPA in a nonlinear medium is typically investigated by measuring it directly at the wavelength of interest, often alongside the nonlinear refractive index (n_2) using techniques such as Z-scan. In our case, direct measurement of n_2 or the TPA coefficient (β) was not feasible, as the technique demands higher laser intensities than those provided by our fs laser.

As an alternative, the possible existence of TPA can be inferred by estimating the optical bandgap of the Kerr medium, in this case, BBS glass, and comparing it with twice the photon energy of the excitation light. If the bandgap corresponds to this value, two-photon absorption is likely to occur. The optical bandgap can be determined using the Tauc plot method [48,49], which analyzes the linear absorption (or transmission) spectrum of amorphous materials. In this approach, the photon energy is plotted against $(\alpha h\nu)^{n}$, where α is the absorption coefficient, $h\upsilon$ is the photon energy, and $n = 2$ for optically allowed direct bandgap, while $n = 1/2$ for indirect bandgaps, as is appropriate for our systems. This method has been successfully applied to various glass systems, including BBS glass with different Bi_2O_3 contents, as demonstrated by Gao et al. [50].

For the OKG measurements, the pump (gate) and probe beams were at a central wavelength of 820 nm with a spectral bandwidth of 15 nm. For TPA to occur, two photons reaching at an optical bandgap corresponding to 3.02 eV (representing 410 nm, which is half the excitation wavelength) must be absorbed simultaneously. The optical bandgap of our BBS glass specimen determined from Tauc plot (see Fig. 3) is $E_g = 2.93$ eV, corresponding to a wavelength of approximately 423 nm; or 2.821 eV (440 nm) when using the empirical formula relating the bandgap to molar refraction. Despite the bandgap wavelength lying below the two-photon range (3.02 eV $\rightarrow$ 410 nm), TPA might be absent or minimal, because the actual bandgap energy is likely larger than 2.93 eV. In fact, the Urbach tail, a combination of the amorphous glass structure and impurities in BBS appear as a lower bandgap [51]. Moreover, the uncertainties of each ingredient used to fabricate the glass specimen are not known, hence the optical bandgap of the BBS glass cannot be precisely obtained within the uncertainty range of the ingredients of its composition, which will slightly shift the E_g to higher or lower value. The result of Eq. (3) does not take into account these facts. Further, in our case TPA would be a minor contributor to heat accumulation, as compared to linear absorption, which is within the range of 25-32% as we pointed out earlier.

The gate efficiency attained in this work (~ 3%) was obtained using a CW laser probe and fs pulsed pump laser, in counter-propagation geometry. Nonetheless, calculation based on a model considering focused beam diffraction and pump and probe pulse co-propagation yields a transmission through the cross polarizers of the order of 15% for 3-mm thick BBS glass and 0.8 nJ pulse energy [34]. However, in this work we are primarily interested in the time resolution as the efficiency can be readily increased by optimizing the experimental parameters, such as the laser power, the degree of ellipticity, or the glass thickness. Even with such gating efficiency, a hybrid quantum system (a quantum emitter coupled to a nanophotonic structure, i.e., gold nanocone) that reaches nearly up to 80% quantum yield, pumped with a 1 GHz repetition rate

Optics EXPRESS

laser, would lead to a count rate of few MHz on the detector, assuming 30% collection efficiency, and 40% detection efficiency (by SPADs). This count rate would be sufficient to apply this OKG for single-photon detection.

Single-photon detection via optical Kerr gating (OKG) has been demonstrated in both single-mode fibers (SMFs) [52] and photonic crystal fibers (PCFs) [53] at low gate pulse energies; however, these platforms remain complex to implement. In both cases, the high confinement of the gate beam's electromagnetic field often induces a spectral background via SPM, which can obscure single-photon signals. While PCFs offer sub-ps temporal resolution, they require specialized dispersion engineering for specific wavelengths, which limits their versatility in real-world applications. Conversely, SMFs have yet to achieve sub-ps resolution, and increasing their length introduces problematic group velocity dispersion and mismatch. Furthermore, despite near-unity transmission, these fiber-based systems suffer from significant total losses ranging between 50–70%, due to low coupling efficiencies into the fibers.

5. Conclusion

To conclude, we have implemented an ultrafast detection scheme based on the third-order nonlinearity of BBS glass, operating at a 1 GHz repetition rate under focusing with less than 1 nJ pulse energy (~ 1.20 GW/cm^2 gate pulse peak intensity), and achieving an instrument response function with a time resolution of 175 fs. BBS glass was chosen for its large nonlinear coefficient, which enhances detection efficiency, and is necessary for operating at high repetition rates, its sub-ps response time, and its compatibility with standard microscopy platforms. This approach potentially provides a robust platform for probing ultrafast photodynamics at the single-emitter level and holds promise for applications in ultrafast single-photon detection, quantum information processing, high-speed optical switching, and time-resolved spectroscopy in nanophotonic and biological systems.

Funding. University of Siegen; Deutsche Forschungsgemeinschaft (INST 221/118-1 FUGG, 410405168).

Acknowledgment. The authors would like to acknowledge Paolo Foggi. Thomas Lenzer, Kawon Oum, and Giancarlo Soavi for helpful discussion and Mauro Pucci for BBS glass polishing.

Disclosures. Authors state no conflict of interest.

Data availability. Data underlying the results presented in this paper are not publicly available at this time but may be obtained from the authors upon reasonable request.

Supplemental document. See Supplement 1 for supporting content.

References

1. Y. Arakawa and M. J. Holmes, "Progress in quantum-dot single photon sources for quantum information technologies: A broad spectrum overview," Appl. Phys. Rev. **7**(2), 021309 (2020).
2. V. Shcheslavskiy, P. Morozov, A. Divochiy, *et al.*, "Ultrafast time measurements by time-correlated single photon counting coupled with superconducting single photon detector," Rev. Sci. Instrum. **87**(5), 053117 (2016).
3. S. Chan, A. Halimi, F. Zhu, *et al.*, "Long-range depth imaging using a single-photon detector array and non-local data fusion," Sci. Rep. **9**(1), 8075 (2019).
4. L. Ma, O. Slattery, and X. Tang, "Single photon frequency up-conversion and its applications," Phys. Rep. **521**(2), 69–94 (2012).
5. E. M. H. P. van Dijk, J. Hernando, J.-J. García-López, *et al.*, "Single-Molecule Pump-Probe Detection Resolves Ultrafast Pathways in Individual and Coupled Quantum Systems," Phys. Rev. Lett. **94**(7), 078302 (2005).
6. Y. Venkatesh, M. Venkatesan, B. Ramakrishna, *et al.*, "Ultrafast Time-Resolved Emission and Absorption Spectra of meso-Pyridyl Porphyrins upon Soret Band Excitation Studied by Fluorescence Up-Conversion and Transient Absorption Spectroscopy," J. Phys. Chem. B **120**(35), 9410–9421 (2016).
7. H. Kandori, H. Sasabe, and M. Mimuro, "Direct Determination of a Lifetime of the S_2 State of beta-Carotene by Femtosecond Time-Resolved Fluorescence Spectroscopy," J. Am. Chem. Soc. **116**(6), 2671–2672 (1994).
8. X.-W. Chen, M. Agio, and V. Sandoghdar, "Metallodielectric Hybrid Antennas for Ultrastrong Enhancement of Spontaneous Emission," Phys. Rev. Lett. **108**(23), 233001 (2012).
9. T. B. Hoang, G. M. Akselrod, and M. H. Mikkelsen, "Ultrafast Room-Temperature Single Photon Emission from Quantum Dots Coupled to Plasmonic Nanocavities," Nano Lett. **16**(1), 270–275 (2016).

Optics EXPRESS

10. A. M. Flatae, F. Tantussi, G. C. Messina, *et al.*, "Plasmon-Assisted Suppression of Surface Trap States and Enhanced Band-Edge Emission in a Bare CdTe Quantum Dot," J. Phys. Chem. Lett. **10**(11), 2874–2878 (2019).
11. S. I. Bogdanov, O. A. Makarova, X. Xu, *et al.*, "Ultrafast quantum photonics enabled by coupling plasmonic nanocavities to strongly radiative antennas," Optica **7**(5), 463 (2020).
12. B. Schmidt, S. Laimgruber, W. Zinth, *et al.*, "A broadband Kerr shutter for femtosecond fluorescence spectroscopy," Appl. Phys. B **76**(8), 809–814 (2003).
13. S. Kinoshita, H. Ozawa, Y. Kanematsu, *et al.*, "Efficient optical Kerr shutter for femtosecond time-resolved luminescence spectroscopy," Rev. Sci. Instrum. **71**(9), 3317–3322 (2000).
14. C. H. Kim and T. Joo, "Ultrafast time-resolved fluorescence by two photon absorption excitation," Opt. Express **16**(25), 20742 (2008).
15. O. Kuzucu, F. N. C. Wong, S. Kurimura, *et al.*, "Time-resolved single-photon detection by femtosecond upconversion," Opt. Lett. **33**(19), 2257 (2008).
16. C. Cimpean, V. Groenewegen, V. Kuntermann, *et al.*, "Ultrafast exciton relaxation dynamics in silicon quantum dots," Laser & Photonics Reviews **3**(1-2), 138–145 (2009).
17. P. Henzler, C. Traum, M. Holtkemper, *et al.*, "Femtosecond Transfer and Manipulation of Persistent Hot-Trion Coherence in a Single CdSe/ZnSe Quantum Dot," Phys. Rev. Lett. **126**(6), 067402 (2021).
18. W. Becker, *The Bh TCSPC Handbook*, 8th ed. Becker & Hickl GmbH, 2019.
19. B. A. Korzh, Q-Y. Zhao, S. Frasca, *et al.*, "Demonstration of sub-3 ps temporal resolution with a superconducting nanowire single-photon detector," Nat. Photonics **14**(4), 250–255 (2020).
20. J. Wiersig, C. Gies, F. Jahnke, *et al.*, "Direct observation of correlations between individual photon emission events of a microcavity laser," Nature **460**(7252), 245–249 (2009).
21. M. Aßmann, F. Veit, M. Bayer, *et al.*, "Ultrafast tracking of second-order photon correlations in the emission of quantum-dot microresonator lasers," Phys. Rev. B **81**(16), 165314 (2010).
22. M. Aßmann, F. Veit, J.-S. Tempel, *et al.*, "Measuring the dynamics of second-order photon correlation functions inside a pulse with picosecond time resolution," Opt. Express **18**(19), 20229 (2010).
23. M. Sajadi, M. Quick, and N. P. Ernsting, "Femtosecond broadband fluorescence spectroscopy by down- and up-conversion in ß-barium borate crystals," Appl. Phys. Lett. **103**(17), 173514 (2013).
24. L. Zhang, Y.-T. Kao, W. Qiu, *et al.*, "Femtosecond Studies of Tryptophan Fluorescence Dynamics in Proteins: Local Solvation and Electronic Quenching," J. Phys. Chem. B **110**(37), 18097–18103 (2006).
25. R. Jimenez, G. R. Fleming, P. V. Kumar, *et al.*, "Femtosecond solvation dynamics of water," Nature **369**(6480), 471–473 (1994).
26. A. Barth, "Infrared spectroscopy of proteins," Biochimica et Biophysica Acta (BBA) - Bioenergetics **1767**(9), 1073–1101 (2007).
27. M. Glasbeek and H. Zhang, "Femtosecond Studies of Solvation and Intramolecular Configurational Dynamics of Fluorophores in Liquid Solution," Chem. Rev. **104**(4), 1929–1954 (2004).
28. H. Chosrowjan, S. Taniguchi, N. Mataga, *et al.*, "Low-Frequency Vibrations and Their Role in Ultrafast Photoisomerization Reaction Dynamics of Photoactive Yellow Protein," J. Phys. Chem. B **108**(8), 2686–2698 (2004).
29. J. Xu and J. R. Knutson, "*Ultrafast Fluorescence Spectroscopy via Upconversion: Applications to Biophysics, In Editors, Methods in Enzymology (1st Ed.)*," Academic Press 450, Volume 450Chap. 8, 159–183 (2008).
30. Z. Yu, L. Gundlach, and P. Piotrowiak, "Efficiency and temporal response of crystalline Kerr media in collinear optical Kerr gating," Opt. Lett. **36**(15), 2904 (2011).
31. A. Bartels, D. Heinecke, S. A. Diddams, *et al.*, "10-GHz Self-Referenced Optical Frequency Comb," Science **326**(5953), 681 (2009).
32. C. Kerse, H. Kalaycioglu, P. Elahi, *et al.*, "Ablation-cooled material removal with ultrafast bursts of pulses," Nature **537**(7618), 84–88 (2016).
33. S.-W. Chu, T.-M. Liu, C.-K. Sun, *et al.*, "Real-time second-harmonic-generation microscopy based on a 2-GHz repetition rate Ti:sapphire laser," Opt. Express **11**(8), 933–938 (2003).
34. A.-H. Fattah, A. M. Flatae, A. Farrag, *et al.*, "Ultrafast single-photon detection at high repetition rates based on optical Kerr gates under focusing," Opt. Lett. **46**(3), 560 (2021).
35. N. Sugimoto, H. Kanbara, S. Fujiwara, *et al.*, "Third-order optical nonlinearities and their ultrafast response in Bi_2O_3–B_2O_3–SiO_2 glasses," J. Opt. Soc. Am. B **16**(11), 1904 (1999).
36. N. Sugimoto, K. Hirao, H. Kanbara, *et al.*, "Ultrafast response of third-order optical nonlinearity in glasses containing Bi_2O_3," Opt. Lett. **21**(20), 1637 (1996).
37. V. Dimitrov and T. Komatsu, "An interpretation of optical properties of oxides and oxide glasses in terms of the electronic ion polarizability and average single bond strength," J. Univ. Chem. Technol. Metall. **45**(3), 219–250 (2010).
38. V. Dimitrov and T. Komatsu, "Optical basicity and chemical bonding of Bi_2O_3 containing glasses," J. Non-Cryst. Solids **382**(0), 18–23 (2013).
39. J. A. Duffy, "Chemical bonding in the oxides of the elements: A new appraisal," J. Solid State Chem. **62**(2), 145–157 (1986).
40. X. Zhu, C. Mai, and M. Li, "Effects of B_2O_3 content variation on the Bi ions in Bi_2O_3–B_2O_3–SiO_2 glass structure," J. Non-Cryst. Solids **388**, 55–61 (2014).

Optics EXPRESS

41. R. M. Osgood, N. C. Panoiu, J. I. Dadap, *et al.*, "Engineering nonlinearities in nanoscale optical systems: physics and applications in dispersion-engineered silicon nanophotonic wires," Adv. Opt. Photonics **1**(1), 162–235 (2009).
42. T. Lin, Q. Yang, J. Si, *et al.*, "Ultrafast nonlinear optical properties of Bi_2O_3–B_2O_3–SiO_2 oxide glass," Opt. Commun. **275**(1), 230–233 (2007).
43. N. Sugimoto, S. Ito, S. Fujiwara, *et al.*, "Femtosecond and terahertz optical Kerr shutter switching in glass containing high concentration of Bi_2O_3," Opt. Commun. **161**(1-3), 47–50 (1999).
44. W. Tan, H. Liu, J. Si, *et al.*, "Control of the gated spectra with narrow bandwidth from a supercontinuum using ultrafast optical Kerr gate of bismuth glass," Appl. Phys. Lett. **93**(5), 051109 (2008).
45. L. Yan, J. Si, F. Chen, *et al.*, "Pump power dependence of Kerr signals in femtosecond cross pump-probe optical Kerr measurements," Opt. Express **17**(24), 21509 (2009).
46. T. Hasegawa, T. Nagashima, and N. Sugimoto, "Z-scan study of third-order optical nonlinearities in bismuth-based glasses," Opt. Commun. **250**(4-6), 411–415 (2005).
47. J. Zhang, Q. Nie, S. Dai, *et al.*, "Nonlinear optical properties in bismuth-based glasses," J. Wuhan Univ. Technol.-Mat. Sci. Edit. **26**(1), 61–64 (2011).
48. J. Tauc, R. Grigorovici, and A. Vancu, "Optical Properties and Electronic Structure of Amorphous Germanium," Physica Status Solidi (b) **15**(2), 627–637 (1966).
49. J. Tauc, "Optical properties and electronic structure of amorphous Ge and Si," Mater. Res. Bull. **3**(1), 37–46 (1968).
50. Y. Gao, J.-J. Ma, Y. Chen, *et al.*, "Effect of Bi_2O_3 on the structure and thermal properties of Bi_2O_3-SiO_2-$B2O_3$ glasses prepared by sol-gel method," J. Sol-Gel Sci. Technol. **103**(3), 713–721 (2022).
51. D. Möncke and D. Ehrt, "Charge transfer transitions in glasses - Attempt of a systematic review," Optical Materials: X **12**, 100092 (2021).
52. C. Kupchak, J. Erskine, D. England, *et al.*, "Terahertz-bandwidth switching of heralded single photons," Opt. Lett. **44**(6), 1427–1430 (2019).
53. M. Yabuno, T. Takumi, F. China, *et al.*, "Ultrafast measurement of a single-photon wave packet using an optical kerr gate," Opt. Express **30**(4), 4999–5007 (2022).